Effect of Print Orientation and Post-Curing on the Properties of Parts Produced by Digital Light Processing

https://doi.org/10.15255/KUI.2026.035
KUI-48/2026
Original scientific paper
Received June 15, 2026
Accepted July 24, 2026

M.-P. Marković,* *L. Štorga*, *E. Forjan*, and *D. Vrsaljko*
University of Zagreb Faculty of Chemical Engineering and Technology,
Trg Marka Marulića 19, 10 000 Zagreb, Croatia

This work is licensed under a Creative Commons Attribution 4.0 International License

Abstract

Additive manufacturing (3D printing) is a layer-by-layer fabrication technique that enables the production of complex geometries from digital computer-aided design (CAD) models. In digital light processing (DLP) technology, the model is converted into sliced layers and manufactured by the selective photopolymerisation of a liquid resin using projected light.

This study investigates how processing conditions and post-curing influence the properties of an acrylate-based photopolymer resin (AnyCubic 3D Printing UV Sensitive Resin) used in DLP 3D printing. The effects of printing orientation (0°, 45°, and 90°) and post-curing duration (0, 5, and 15 min) in a 405 nm chamber were analysed in terms of mechanical performance, thermal response, and chemical resistance.

The experimental results indicated that printing orientation and post-curing time play a significant role in determining the mechanical and chemical behaviour of the material. Samples printed at 90° relative to the print bed exhibited the highest tensile strength (53.9 MPa) and fracture resistance (53.3 MPa), whereas 0° oriented samples showed the highest Young's modulus (1184 MPa). Solvent uptake was highest in acetone (11 %) and methanol (10 %), and decreased with post-curing time. Thermal analysis showed only minor changes in glass transition temperature (49.1–53.5 °C), while FTIR spectra revealed no significant differences related to post-curing conditions. Overall, the findings highlighted that mechanical and chemical properties of DLP-printed structures can be effectively tuned through printing orientation and post-curing strategy, while thermal properties remain unaffected.

Keywords

Additive manufacturing, digital light processing, printing orientation, post-curing

1 Introduction

Polymers are widely used in medicine, electronics, construction, automotive engineering, and numerous other industrial applications due to their versatility and tuneable properties.[1,2] Among thermosetting polymers, acrylate resins are particularly important because of their excellent mechanical properties, chemical resistance, thermal stability, and dimensional integrity. These characteristics make acrylate-based materials attractive for advanced manufacturing applications, including additive manufacturing.[3,4]

Over the past decade, additive manufacturing (AM) technologies have evolved into advanced manufacturing methods capable of producing complex three-dimensional structures directly from digital models.[5] Their ability to fabricate geometrically complex components with reduced material waste and minimal tooling requirements has led to implementation in aerospace, automotive, biomedical, and consumer applications.[6,7]

Among various AM technologies, vat photopolymerisation (VP) techniques such as stereolithography (SLA) and digital light processing (DLP) have attracted considerable attention because of their high dimensional accuracy.[8] In DLP printing, a projected light source selectively cures liquid photopolymer resin layer by layer, enabling rapid fabrication while maintaining high precision and repeatability. Compared to conventional SLA, DLP enables faster fabrication while maintaining high precision and repeatability.[9,10] The composition of the resin significantly influences its processing behaviour and final material properties. The ratio of monomers to oligomers affects the resin viscosity, printability, and mechanical performance of the cured material, while the concentration of photoinitiators plays a key role in achieving efficient and uniform curing. The final properties of printed components are influenced by both the resin formulation and processing parameters, including printing orientation and post-curing conditions.[11]

* Corresponding author: Marijan-Pere Marković, PhD
e-mail: mmarkovi1@fkit.unizg.hr

Due to limited exposure time during printing, complete polymerisation is often not achieved, leaving a fraction of uncured resin within the polymer network.[12] For this reason, post-curing treatments are commonly applied to increase the degree of conversion and improve the mechanical, thermal, and chemical properties of printed parts. These processes, typically based on UV or thermal treatment, are strongly influenced by parameters such as exposure time, wavelength, and printing orientation, which affect crosslink density, tensile behaviour, thermal stability, and solvent resistance.[13,14] In particular, irradiation at 405 nm has been widely reported as effective for achieving efficient curing and enhanced mechanical performance in DLP-printed photopolymers.[15,16]

To the authors' knowledge, this is one of the few studies that investigates the combined effect of printing orientation and post-curing time on the mechanical, thermal, chemical, and structural properties of a commercial acrylate-based DLP photopolymer resin.[17] Previous studies have separately investigated the effects of printing orientation or post-curing conditions on the mechanical performance of DLP-printed photopolymers; however, comprehensive studies combining mechanical, swelling, thermal, and spectroscopic characterisation for commercial acrylate-based resins remain limited.

A previous study by *Cingesar et al*.[18] investigated the influence of printing parameters, including printing angle and layer thickness, together with different post-curing conditions, on the mechanical, thermal, and physicochemical properties of two acrylate resins fabricated using stereolithography (SLA). Building on this work, the present study focuses on a commercial acrylate-based resin fabricated using digital light processing (DLP) and systematically evaluates the combined effects of printing orientation and defined post-curing durations. Although the influence of printing orientation and post-curing on photopolymer properties has previously been investigated, further studies combining mechanical, swelling, thermal, and spectroscopic characterisation of commercial acrylate-based resins fabricated by DLP remain relevant.

The aim of this study was to investigate the influence of printing orientation (0°, 45° and 90°) and post-curing time (0, 5 and 15 min) in a 405 nm chamber on the mechanical, thermal, and chemical properties of acrylate-based resins fabricated using DLP 3D-printing technology. Mechanical properties were evaluated using tensile testing, thermal behaviour was analysed by differential scanning calorimetry (DSC), while chemical resistance was assessed through swelling tests in water, acetone, and methanol. Additionally, Fourier-transform infrared spectroscopy (FTIR) was employed for structural characterisation of the printed samples.

2 Experimental

2.1 Materials

An acrylate-based commercial photopolymer resin (AnyCubic 3D Printing UV Sensitive Resin, AnyCubic, China) was used in this study. The resin is specifically designed for additive manufacturing applications using DLP/SLA 3D-printing technologies. According to the manufacturer's technical data sheet, the resin exhibits a tensile strength of 40–50 MPa, a Young's modulus of 1600–1800 MPa, an elongation at break of 12–16 % (method not specified), a hardness of 84 Shore D, a density of 1.13 $g\,cm^{-3}$, and a viscosity of 200–230 mPa s at 25 °C. The AnyCubic UV-sensitive resin is a photopolymer formulation typically composed of multifunctional acrylate/methacrylate monomers and oligomers as the main resin matrix. The organic phase generally consists of approximately 40–70 % acrylate/methacrylate oligomers and 20–50 % reactive monomers, which provide the crosslinking network upon irradiation exposure. A small fraction (< 5 %) of photoinitiators is included to enable radical generation, initiating the polymerisation, enabling rapid curing of individual layers during the printing process. The resin is characterised by low viscosity and efficient curing behaviour, which, together with the high printing precision of DLP technology, enable the fabrication of fine features and complex geometries with dimensional accuracy and surface quality.

2.2 3D printing

The 3D models of the test samples were designed using a computer-aided design (CAD) software Autodesk Fusion. Type 5B tensile sample was created in accordance with the ISO 527-2:2025 standard.[19] After completion of the design, the model was exported in STL format. Prior to printing, the STL models were processed using Chitubox V1.9.4, where the printing orientation and process parameters were defined. This software enables control of key printing parameters such as layer thickness (0.05 mm), printing orientation (0°, 45°, 90°) and exposure time (2.6 s). It also allows the generation and optimisation of support structures. In addition, batch printing was employed, enabling the simultaneous fabrication of five tensile samples ($n = 5$) in a single print job. The sample designated as 0° was printed in a horizontal orientation, while the 45° and 90° samples were printed at the corresponding angles relative to the build platform. A slight inclination was introduced for the nominally 0° orientation to facilitate resin drainage from the sample surface and improve the removal of excess resin during fabrication. This modification did not alter the defined 0° printing orientation or the orientation of the printed layers relative to the tensile loading direction. For each printing orientation (0°, 45°, and 90°), a total of 15 samples were fabricated ($n = 15$). The samples were divided into three experimental groups ($n = 5$ *per* group):

without post-curing, post-cured for 5 min, and post-cured for 15 min. All samples were first subjected to tensile testing. Subsequently, fragments obtained from the fractured tensile samples were used for the DSC and FTIR analyses. This approach ensured that all characterisation techniques were performed on material originating from the same samples. Swelling measurements were performed using separately printed samples with dimensions of $20 \times 10 \times 2$ mm. After fabrication, all printed samples were removed from the build platform, cleaned, and assigned a unique identification number. The samples were labelled and stored separately in clearly marked zip-lock bags throughout the experimental procedure. This identification system was maintained during all subsequent post-curing and characterisation steps to ensure complete traceability and prevent sample misidentification. DLP 3D printer Anycubic Photon M3 (Anycubic, China) was used for the fabrication of tensile samples. Samples were fabricated at different build orientations (0°, 45°, and 90°) relative to the printing platform.

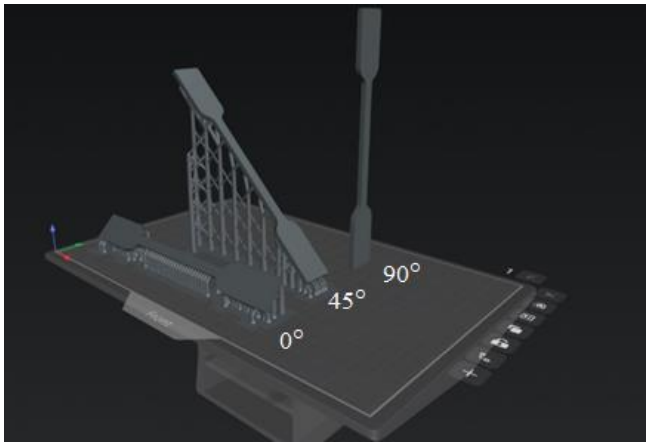


Fig. 1 – Arrangement of sample models for all printing orientations (0°, 45°, and 90°) in Chitubox software

Slika 1 – Prikaz modela epruveta za sve orijentacije ispisa (0°, 45° i 90°) u programu Chitubox

2.3 Post-curing

Following the printing process, the s were immersed in isopropyl alcohol (IPA) to remove residual uncured resin, and were subsequently subjected to additional curing treatment. Post-curing was carried out using a 405 nm curing chamber Anycubic Wash & Cure 3 (Anycubic, China), which provided controlled 405 nm exposure for further curing of the printed material. The samples were cured for 0, 5, and 15 min.

2.4 Mechanical properties

The mechanical properties of the printed samples were evaluated using a universal testing machine (UTM 1445, Zwick/Roell, Germany). The initial gauge length (20 mm) and the crosshead speed (10 mm min^{-1}) were selected in accordance with ISO 527-2:2025 for Type 5B tensile samples. The test was controlled, and the data were acquired using test Xpert software. At least five samples ($n = 5$) were tested for each experimental condition to obtain representative and reproducible results. The reported mechanical properties represent the average values calculated from the tested samples and are expressed as mean ± standard deviation.

2.5 Thermal properties

Thermal characterisation of the prepared samples was performed using a DSC 823^e differential scanning calorimeter (Mettler Toledo, Switzerland). For each measurement, a small fragment was cut from the fractured tensile sample after mechanical testing. Approximately 10 mg of material was used for each analysis. The exact sample mass was recorded prior to testing, and the DSC heat flow data were normalised to the sample mass using the instrument STARe software. Measurements were conducted in aluminium sample pans. All experiments were performed under a continuous nitrogen atmosphere with a flow rate of 50 ml min^{-1} to ensure inert testing conditions and minimise possible oxidative effects. The samples were first cooled from room temperature to 0 °C, followed by a stabilisation period (2 min) at constant temperature. The materials were then heated to 250 °C at a controlled heating rate (10 °C min^{-1}). After the heating cycle, the samples were cooled back to room temperature at a rate of −30 °C min^{-1}.

2.6 Chemical and structural analysis

The chemical structure of the acrylate-based resin samples was investigated using Fourier-transform infrared spectroscopy (FTIR). FTIR measurements were carried out using a PerkinElmer Spectrum One spectrometer equipped with an attenuated total reflectance (ATR) accessory. Fragments obtained from the fractured tensile samples after mechanical testing were analysed without additional sample preparation. One representative sample ($n = 1$) was analysed for each post-curing condition, as the objective of the FTIR analysis was to identify the characteristic functional groups and evaluate chemical changes induced by post-curing. Since the printing orientation was not expected to affect the chemical composition of the resin, FTIR measurements were not repeated for all printing orientations and were performed only on representative samples. The obtained

infrared spectra were used to identify characteristic absorption bands and corresponding functional groups of the analysed resin samples, as well as to evaluate molecular vibrations associated with the polymer network structure. FTIR spectra were recorded over the range 4000–650 cm^{-1} with a spectral resolution of 4 cm^{-1}.

2.7 Physicochemical properties

The chemical resistance of the printed samples was evaluated by swelling experiments performed in different solvents. Dedicated samples with dimensions of 20 × 10 × 2 mm (n = 1, for each printing orientation and post-curing condition) were used for the swelling measurements. Prior to immersion, the initial mass of each sample was recorded. The samples were immersed separately in water, acetone, and methanol at room temperature. A sufficient volume of each solvent was used to ensure complete immersion of the samples. Before each weighing, the sample was gently placed on absorbent paper to remove the excess solvent adhering to the surface without applying pressure, after which it was immediately weighed. The degree of swelling was determined gravimetrically by monitoring the mass change of the samples during solvent exposure. The swelling behaviour was calculated from the difference between the initial sample mass and the mass measured after a defined immersion period according to Eq. (1):

$$swelling\ degree\,(\%) = \frac{m_t - m_0}{m_0} \cdot 100 \qquad (1)$$

where m_0 is the initial mass of the dry sample and m_t is the mass of the sample after immersion for time t.

Water, acetone, and methanol were selected as test solvents in order to investigate the interaction between the polymer network and media of different polarity. The analysis included samples without additional curing treatment, as well as samples post-cured in a 405 nm chamber for 5 and 15 min. The measurements were performed to evaluate solvent resistance and to determine the influence of post-curing time on the chemical stability of the acrylate-based resin. During the swelling experiments, the mass of each sample was recorded after 15, 30, 60, 120, and 240 min, as well as after 1440 min of immersion.

3 Results and discussion

3.1 Mechanical properties

The mechanical properties of the samples were evaluated using tensile testing on a universal testing machine. The obtained results (Table 1) included tensile strength (σ_M), strain at tensile strength (ε_M), stress at break (σ_R), strain at break (ε_R), Young's modulus (E), and work (W).

The layer thickness was 0.05 for all samples. Sample designations consisted of ACC (AnyCubic Clear) + curing time (0, 5 and 15 min) + printing orientation (0°, 45° and 90°). The printing orientations were defined with respect to the build platform, where 0° corresponds to samples printed parallel to the platform, and 90° corresponds to samples printed perpendicular to the platform. The results indicated that the increase in tensile strength observed for samples printed at 90° and post-cured for 15 min suggests improved load transfer efficiency between cured layers and a more favourable orientation relative to the applied tensile force (53.9 MPa).

Table 1 – Tensile test results for the mechanical properties, presented as mean values ± standard deviation, calculated from five tested samples (n = 5) for each experimental condition

Tablica 1– Rezultati ispitivanja mehaničkih svojstava prikazani kao srednje vrijednosti ± standardna devijacija, izračunate na temelju pet ispitanih uzoraka (n = 5) za svaku eksperimentalnu skupinu

Orientation / ° Orijentacija / °	Curing time / min Vrijeme naknadnog očvršćivanja / min	Sample designation Naziv uzorka	σ_M / MPa	ε_M / %	σ_R / MPa	ε_R / %	E / MPa	W / Nm
0	0	ACC000	20.2±1.3	9.0±2.4	19.2±1.9	10.0±1.9	301±51	0.06±0.01
0	5	ACC500	41.2±9.8	4.5±0.9	35.6±11.9	4.9±0.3	966±131	0.05±0.01
0	15	ACC1500	50.6±13.6	4.3±0.8	44.2±5.7	4.9±0.4	1184±53	0.06±0.01
45	0	ACC045	21.8±1.9	11.2±1. 9	21.4±2.1	11.2±1.9	321±45	0.08±0.02
45	5	ACC545	45.7±3.9	4.6±0.3	44.8±1.1	4.8±0.2	1045±28	0.06±0.01
45	15	ACC1545	46.3±2.3	4.8±0.3	39.2±1.7	5.2±0.8	927±516	0.06±0.02
90	0	ACC090	23.7±2.2	15.4±1.9	23.4±1.3	15.5±1.4	300±19	0.11±0.02
90	5	ACC590	47.3±1.5	4.7±0.2	37.0±18.9	5.0±0.6	960±541	0.05±0.02
90	15	ACC1590	53.9±4.9	5.0±0.9	53.3±9.8	5.3±0.9	1039±581	0.06±0.04

In contrast, the highest values of strain at maximum tensile strength and strain at break were observed for samples printed at 90° without post-curing treatment with a value of 15.5 %. The lowest tensile strength (20.2 MPa) was measured for samples printed at 0° without post-curing, whereas the lowest strain at maximum tensile strength (4.3 %) was recorded for 0° samples post-cured for 15 min.

The highest Young's modulus was obtained for samples printed at 0° orientation and post-cured for 15 min (1184 MPa), whereas the lowest Young's modulus (300 MPa) was observed for samples printed at 90° without additional post-curing.

The highest work fracture was recorded for samples printed at 90° without post-processing (0.11 N m). In contrast, samples printed at both 0° and 90° and post-cured for 5 min exhibited the same work of fracture (0.05 N m).

Samples fabricated at a 90° printing orientation exhibited higher tensile strength and work of fracture compared to samples printed at lower orientations. Similar observations regarding the influence of build orientation on the mechanical performance of vat-photopolymerised materials have been reported in previous studies.[16,17] The superior mechanical performance observed for the 90° printed samples is not unexpected. In addition to the effect of sample orientation and layer arrangement, the printing angle influences the exposure conditions during the layer-by-layer photopolymerisation process. Samples printed at different orientations experienced different irradiation histories during fabrication. The 0° orientation was associated with a shorter light exposure path and lower cumulative irradiation time compared with vertically oriented samples, whereas the 90° orientation required a longer printing sequence and consequently may receive a higher cumulative UV exposure during fabrication. This extended exposure may promote a higher degree of polymer network formation and reduced residual uncured resin content, resulting in improved tensile strength and Young's modulus. Differences in the relative arrangement of the printed layers and the applied tensile load may also contribute to the observed mechanical trends. In this context, the lower tensile strength and work of fracture observed for the 0° samples may be related to differences in the way the printed structure transfers the applied load. However, the present study did not include dedicated fractographic analysis, and the observed fracture appearance was predominantly brittle and similar among the investigated samples. Therefore, specific fracture mechanisms, such as preferential failure along interlayer regions, could not be directly confirmed from the present data. Samples printed at 0° generally demonstrated lower tensile strength and lower work of fracture, indicating lower toughness, while at the same time exhibiting the highest Young's modulus.

In addition to printing orientation, the duration of post-curing in the 405 nm chamber significantly influenced the mechanical response. Samples without post-curing or with shorter curing times showed lower strength and stiffness but higher elongation and work of fracture, indicating increased ductility compared to samples with extended post-curing times. Similar trends were reported by *Wang et al.*[20], who observed increased tensile strength and stiffness after extended post-curing of SLA/DLP printed materials. Such behaviour indicates the formation of a more densely crosslinked polymer network during prolonged irradiation exposure. Increased crosslink density restricts molecular mobility, thereby improving stiffness and strength while simultaneously reducing ductility and toughness.

These trends can be explained by the increase in the degree of crosslinking with longer irradiation exposure. A higher crosslink density leads to improved mechanical strength due to the formation of additional covalent bonds that reinforce the polymer network and resist deformation. However, increased crosslinking also reduces chain mobility, resulting in decreased elasticity and lower elongation at break. This behaviour is characteristic of highly crosslinked thermoset polymers.[21]

Figs. 2, 3, and 4 show the representative curves for samples printed at orientations of 0°, 45°, and 90°. The figures include samples without post-curing as well as samples subjected to additional post-curing in a 405 nm chamber for 5 and 15 min.

Sample designations are ACC (acrylate component) + curing time (0, 5, and 15 min) + printing orientation (0°, 45° and 90°).

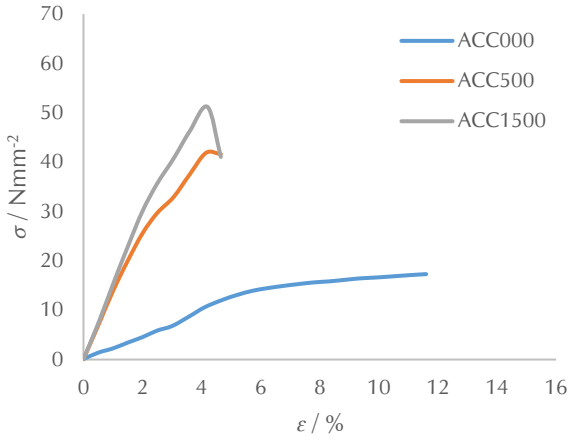


Fig. 2 – Stress–strain curves for samples printed at a 0° orientation, including all post curing conditions (0, 5, and 15 min of irradiation exposure in a 405 nm chamber)

Slika 2 – Grafički prikaz ovisnosti naprezanja o istezanju za epruvete ispisane pod kutom od 0° i sva vremena naknadnog očvršćivanja (0 min, 5 min, 15 min)

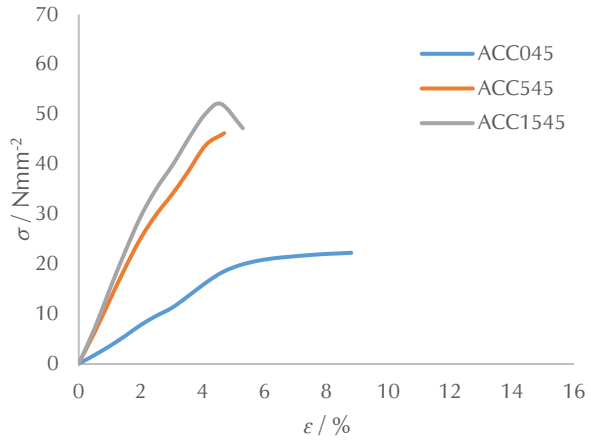


Fig. 3 – Stress–strain curves for samples printed at a 45° orientation, including all post curing conditions (0, 5, and 15 min of irradiation exposure in a 405 nm chamber)

Slika 3 – Grafički prikaz ovisnosti naprezanja o istezanju za epruvete ispisane pod kutom od 45° i sva vremena naknadnog očvršćivanja (0 min, 5 min, 15 min)

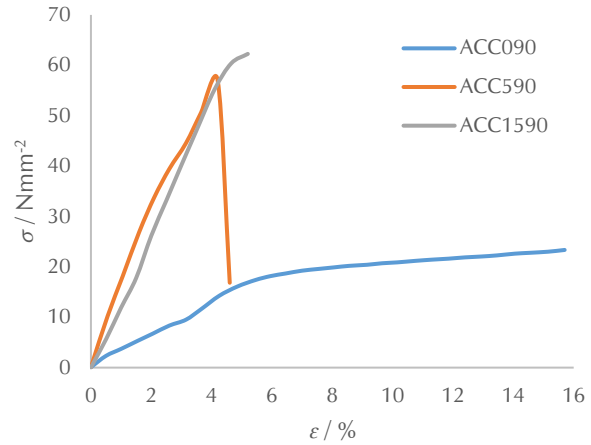


Fig. 4 – Stress–strain curves for samples printed at a 90° orientation, including all post curing conditions (0, 5, and 15 min of irradiation exposure in a 405 nm chamber)

Slika 4 – Grafički prikaz ovisnosti naprezanja o istezanju za epruvete ispisane pod kutom od 90° i sva vremena naknadnog očvršćivanja (0 min, 5 min, 15 min)

Visual inspection of the fractured samples revealed a predominantly brittle fracture appearance, with no obvious macroscopic differences in fracture mode between the investigated printing orientations and post-curing conditions (Fig. 5).

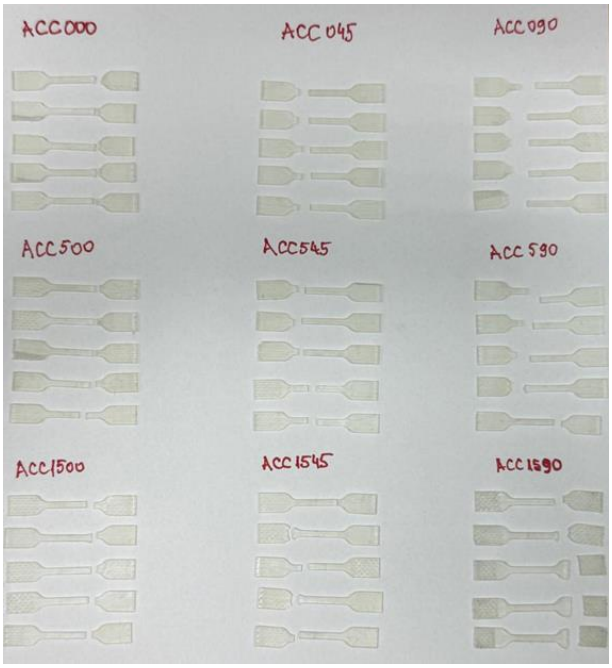


Fig. 5 – All samples after tensile testing

Slika 5 – Svi uzorci nakon provedenog ispitivanja na kidalici

3.2 Thermal properties

DSC analysis was performed to evaluate the thermal properties of AnyCubic UV-sensitive resin samples printed at the same layer thickness (0.05 mm), at different orientations, and subjected to various post-curing times in a 405 nm chamber. The analysis provided several values of the glass transition temperature, including the glass transition temperature (T_g) based on the inflection point ($T_{g,inflect}$), midpoint method ($T_{g,midpoint}$), and the angle midpoint method ($T_{g,anglemidpoint}$). Since the glass transition occurs over a temperature range rather than at a single temperature, different evaluation methods can be used to determine T_g from DSC thermograms. Therefore, T_g values based on the inflection point, midpoint method, and angle midpoint method were evaluated to provide a more comprehensive characterisation of the glass transition behaviour. In addition, the change in heat capacity (Δc_p) and the curing enthalpy (ΔH) of the liquid resin were determined. The results indicate that both the printing orientation and the post-curing conditions influenced the thermal response of the material, particularly the glass transition temperature and Δc_p values.

Slight variations can be observed depending on the method used for T_g determination. For T_g determined by the inflection point method, the lowest values among all printed samples were observed for samples printed at 0° (49.8 °C), 45° (49.1 °C), and 90° (49.1 °C) without post-curing. The highest value (53.5 °C) was recorded for the 90° sample post-cured for 15 min. When considering the

midpoint method in the 0° orientation, the lowest $T_{g,midpoint}$ was observed for the non-post-cured sample (45.7 °C), whereas the highest (46.8 °C) was obtained after 15 minutes of post-curing. For 45° printed samples, the highest $T_{g,midpoint}$ (56.3 °C) was recorded for the non-post-curing sample, while the lowest (46.3 °C) was observed for the 5 min post-cured sample. For the 90° orientation, the highest value (56.3 °C) was observed after the non-post-treatment treatment, and the lowest (46.1 °C) after 5 min post-treatment. According to the angle midpoint method, the lowest T_g (48.6 °C) was measured for 0° samples post-cured for 15 min, while the highest value (53.2 °C) was obtained for 45° non-post-cured samples.

The observed variations in T_g values among different printing orientations are relatively small and are within the range of experimental variability. Therefore, the DSC analysis was not intended to evaluate the influence of printing orientation on thermal behaviour, as no significant differences among orientations were expected based solely on the printing angle. Instead, DSC measurements were performed to evaluate the effect of post-curing time on the thermal properties of the printed resin, including changes associated with additional polymerisation and crosslinking of the polymer network.

The Δc_p values were negative for all investigated samples. The highest Δc_p ($-29.95 \cdot 10^{-3}$ W g^{-1}) was observed for 45° samples post-cured for 15 min , while the lowest value ($-1.16 \cdot 10^{-3}$ W g^{-1}) was recorded for 90° samples without post-curing. Overall, the results show that the differences in glass transition temperature ($T_{g,inflect}$) and Δc_p among the tested samples were increasing, indicating additional crosslinking occurring during the post-treatment. It can be suggested that printing orientation and post-curing time had an influence on the thermal properties of the investigated resin system. For the liquid resin, the enthalpy of complete curing could also be determined, while for the 3D printed samples, this value was no longer fully accessible due to prior polymerisation during the printing process.

3.3 Chemical and structural analysis

FTIR analysis was performed to identify the characteristic functional groups present in the uncured resin and the 3D-printed samples. The spectra confirmed the presence of functional groups typical of acrylate-based photopolymer resins, including hydroxyl (O−H), aliphatic C−H, carbonyl (C=O), aromatic C=C, C−O, and epoxide ring vibrations. These results verify the successful formation of the polymer network after curing, and the observed absorption bands were consistent with the expected chemical structure of the acrylate-based resin. No significant differences were observed among samples subjected to different post-curing times, indicating that no substantial changes in the overall chemical composition or the characteristic functional groups were detectable by the applied FTIR analysis. The possibility of changes in the degree of conversion or crosslink density during post-curing cannot be excluded; however, such changes cannot be directly established from the present qualitative FTIR results alone. The observed changes in thermal behaviour were therefore evaluated separately using DSC analysis. Similar findings have been reported in previous studies.[22]

Table 2 – DSC analysis results
Tablica 2– Rezultati DSC analize

Orientation / ° Orijentacija / °	Curing time / min Vrijeme naknadnog očvršćivanja / min	Sample designation Naziv uzorka	$T_{g,inflect}$ / °C $T_{g\ (točka\ infleksije)}$ / °C	$T_{g,midpoint}$ / °C $T_{g\ (srednja\ točka\ prijelaza)}$ / °C	$T_{g,anglemidpoint}$ / °C $T_{g\ (kutna\ srednja\ točka)}$ / °C	Δc_p / W g^{-1}	ΔH / J g^{-1}
0	0	ACC000	49.8	45.7	49.8	$-3.31 \cdot 10^{-3}$	/
0	5	ACC500	52.0	46.6	50.8	$-16.48 \cdot 10^{-3}$	/
0	15	ACC1500	53.2	46.8	48.6	$-25.64 \cdot 10^{-3}$	/
45	0	ACC045	49.1	56.3	53.2	$-5.89 \cdot 10^{-3}$	/
45	5	ACC545	51.8	46.3	50.1	$-21.27 \cdot 10^{-3}$	/
45	15	ACC1545	53.3	47.9	51.9	$-29.95 \cdot 10^{-3}$	/
90	0	ACC090	49.1	56.3	49.8	$-1.16 \cdot 10^{-3}$	/
90	5	ACC590	52.5	46.1	51.1	$-14.61 \cdot 10^{-3}$	/
90	15	ACC1590	53.5	47.0	50.5	$-19.47 \cdot 10^{-3}$	/
/	0	ACC liquid resin	/	/	/	/	197.05

3.4 Physicochemical properties

Fig. 6 shows the dependence of the swelling degree of resin samples that were not subjected to post-curing in water, acetone, and methanol. Fig. 7 presents the swelling behaviour of samples post-cured for 5 min in a 405 nm chamber in the same solvents, while Fig. 8 illustrates the swelling response of samples post-cured for 15 min under identical conditions. Swelling measurements were performed using one representative sample for each printing orientation and post-curing condition ($n = 1$). Therefore, the reported swelling values represent individual measurements, and experimental variability could not be quantified using standard deviations or error bars. The swelling kinetics were fitted using a second-order polynomial regression model because swelling was monitored at multiple immersion times. The corresponding equations and coefficients of determination (R^2) are provided for the fitted curves. These fits were used to describe the observed time-dependent swelling trends and do not represent a mechanistic diffusion model. The obtained results indicate that all samples exhibited a certain degree of swelling in all tested solvents. After 24 h of immersion, the highest swelling ratios were observed in acetone, followed by methanol, while water showed the lowest degree of penetration into the polymer network. This is reflected in the relatively low swelling values in water, ranging from 0.57 % for samples post-cured for 15 min up to 1.70 % for samples without post-curing treatment. The uncured samples immersed in acetone exhibited extensive swelling, leading to partial fragmentation after 24 h, which prevented determination of the swelling degree. Overall, the results indicate a higher affinity of the acrylate-based resin toward organic solvents, particularly acetone and methanol, whereas water showed limited penetration into the polymer network, consistent with previous findings for acrylate photopolymers.[23] In addition to solvent type, swelling behaviour was strongly influenced by post-curing duration. Solvent uptake decreased with increasing irradiation exposure time, which can be attributed to the higher crosslink density of the polymer network, reducing free volume and restricting solvent diffusion.[14,24,25]

The swelling kinetics also revealed differences in solvent uptake during the immersion period.

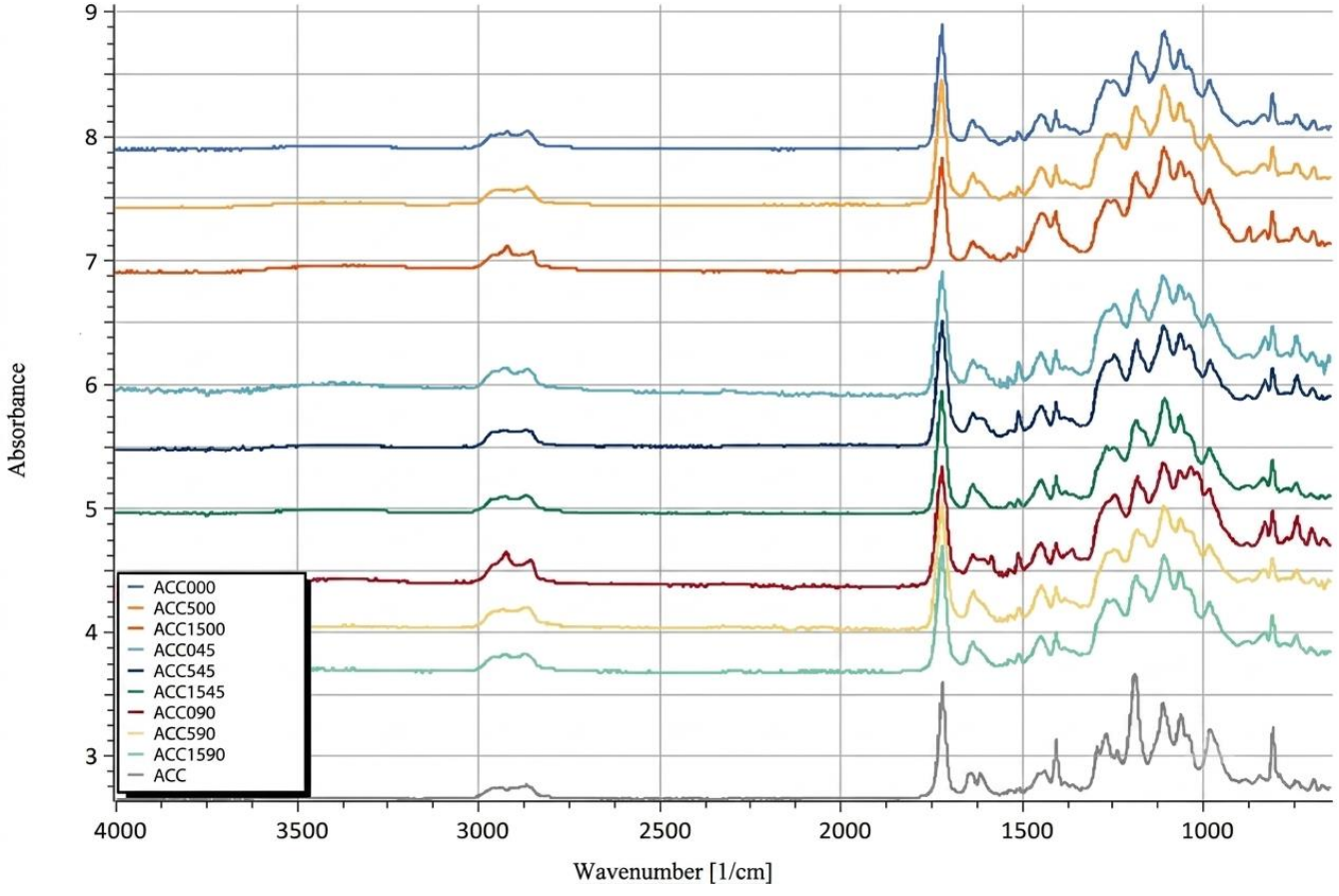


Fig. 6 – Absorbance as a function of wavenumber for all samples

Slika 6 – Grafička ovisnost apsorbancije o valnom broju za sve uzorke

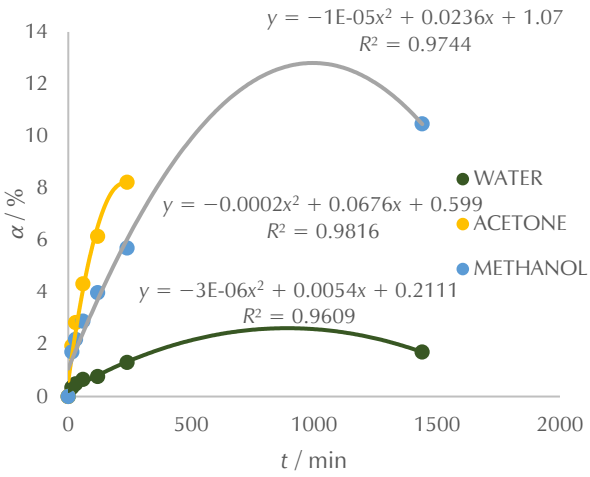


Fig. 7 – Swelling degree in water, acetone, and methanol for non-post-processed samples

Slika 7 – Grafički prikaz ovisnosti stupnja bubrenja u vodi, acetonu i metanolu za uzorke bez post-obrade

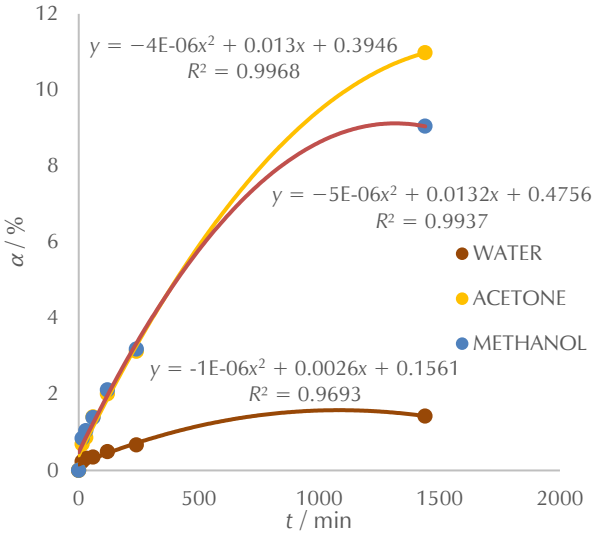


Fig. 8 Swelling degree in water, acetone, and methanol for samples post-cured for 5 min

Slika 8 – Grafički prikaz ovisnosti stupnja bubrenja u vodi, acetonu i metanolu za uzorke koji su naknadno očvršćeni 5 min

The highest changes in sample mass occurred during the initial stages of exposure, indicating rapid solvent diffusion into the accessible free volume of the polymer network. With increasing immersion time, the swelling rate gradually decreased as the system approached equilibrium, suggesting that solvent diffusion became limited by the crosslinked structure. Longer post-curing times reduced the overall swelling response, which may be associated with changes in the polymer network that reduced solvent uptake and restricted solvent diffusion, resulting in lower solvent uptake throughout the immersion period.

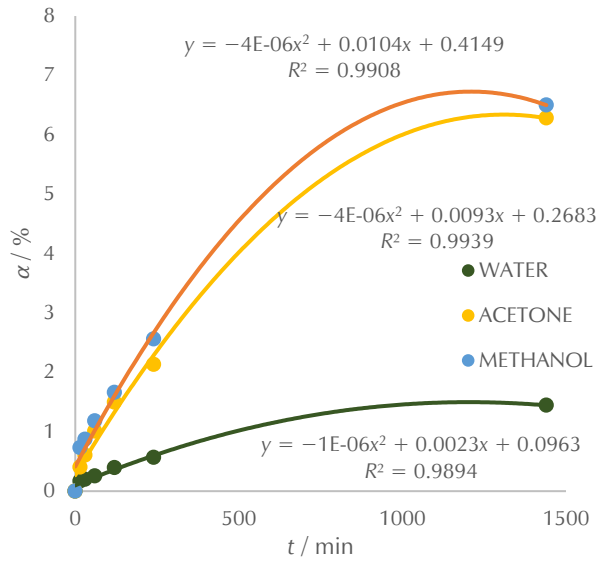


Fig. 9 – Swelling degree in water, acetone, and methanol for samples post-cured for 15 min

Slika 9 – Grafički prikaz ovisnosti stupnja bubrenja u vodi, acetonu i metanolu za uzorke koji su naknadno očvršćeni 15 min

The results demonstrate that both the printing orientation and post-curing treatment influenced the properties of the investigated acrylate-based photopolymer resin, although their effects are reflected in different aspects of material behaviour. The mechanical characterisation showed that samples printed at a 90° orientation exhibited the highest tensile strength after 15 min of post-curing, while those printed without post-curing generally showed higher elongation at break. These findings indicate that the printing orientation affects the mechanical response of the material through differences in the layer arrangement and cumulative UV exposure during the printing process. Samples printed at 90° require a longer layer-by-layer fabrication sequence, which may promote a higher degree of polymer conversion and contribute to improved tensile strength and stiffness. Similar observations have been reported for vat-photopolymerised materials, where the mechanical behaviour depends on both the build orientation and the extent of post-polymerization.[16,17]

The DSC analysis was performed to evaluate the influence of post-curing treatment on the thermal behaviour of the printed resin rather than to assess the effect of printing orientation. Accordingly, only minor differences in glass transition temperature were observed among the investigated

printing orientations, whereas post-curing produced the most pronounced changes in the thermal response. The additional UV exposure during post-curing promoted further polymerisation of residual reactive groups, leading to a higher degree of crosslinking and reduced residual curing potential, consistent with the DSC results.

The swelling experiments further supported these findings. Water caused only limited swelling, whereas acetone and methanol exhibited considerably higher solvent uptake, demonstrating the greater affinity of the acrylate network toward organic solvents. Increasing the post-curing time reduced solvent absorption, which can be attributed to the formation of a denser polymer network with lower free volume and restricted solvent diffusion. The agreement between the DSC and swelling results indicates that the enhanced crosslink density achieved during post-curing improved both the thermal stability and chemical resistance of the printed material.

Overall, the results demonstrate that post-curing was the dominant factor governing the thermal behaviour and chemical resistance of the investigated resin, whereas the printing orientation primarily affected the mechanical properties. The combination of mechanical, thermal, and swelling analyses provided a comprehensive understanding of the relationship between processing conditions and the final performance of DLP-printed acrylate materials.

4 Conclusion

In this study, the effects of printing orientation (0°, 45°, and 90°) and post-curing time (0, 5, and 15 min) on the properties of an acrylate-based resin fabricated by DLP 3D printing were investigated. Mechanical testing showed a strong dependence of tensile behaviour on both processing parameters. The highest tensile strength (σ_M) of 53.3 MPa was obtained for samples printed at 90° and post-cured for 15 min, while the lowest value (19.2 MPa) was recorded for samples printed at 0° without post-curing. The highest strain at break (ε_R) of 15.4 % and work of fracture (W) of 0.11 N m were observed for samples printed at 90° without post-curing, whereas the highest Young's modulus (E) of 1184 MPa was achieved for samples printed at 0° after 15 min of post-curing. Increasing post-curing time improved strength and stiffness but reduced deformability and fracture resistance. Swelling experiments demonstrated that solvent uptake depended strongly on both the solvent type and post-curing conditions. The highest swelling degree was observed in acetone (11 %), followed by methanol (10 %), while water exhibited the lowest uptake (1.7 %). Prolonged post-curing reduced solvent absorption in all tested media, indicating improved solvent resistance, consistent with the formation of a more highly crosslinked polymer network. The DSC analysis was performed to evaluate the effect of post-curing on the thermal behaviour of the printed resin. DSC analysis revealed variations in glass transition temperature among the investigated samples, with T_g values ranging from 45.7 to 56.3 °C, while only minor differences were observed among the investigated printing orientations. The observed changes in thermal behaviour following post-curing may be associated with continued polymerisation or changes in the polymer network during post-treatment; however, the present results do not allow the crosslink density to be directly quantified. FTIR analysis confirmed the presence of characteristic functional groups of the acrylate-based resin and showed no significant differences among post-curing conditions. Overall, the results demonstrate that printing orientation and post-curing can be effectively used to tailor the mechanical performance and solvent resistance of DLP-printed acrylate-based components. This study provides a correlation between processing conditions, mechanical behaviour, swelling response, thermal properties, and chemical structure, contributing to the optimisation of processing parameters for acrylate-based photopolymer resins in DLP additive manufacturing.

ACKNOWLEDGEMENTS

This work was supported by the Croatian Science Foundation under the project numbers HRZZ DOK-2025-02-4318, HRZZ DOK-NPOO-2023-10-1144, HRZZ-DOK-2021-02-5999, and HRZZ IP 2022-10-8004.

References
Literatura

1. *G. Odian*, *Principles of Polymerization*, 4; Wiley-Interscience: Hoboken, NJ, USA, 2004.
2. *W. D. Callister*, *D. G. Rethwisch*, Materials Science and Engineering: An Introduction, 9, Wiley: New York, USA, 2014.
3. *C. A. May*, *Epoxy Resins: Chemistry and Technology*, Marcel Dekker: New York, USA, 1988.
4. *E. M. Petrie*, Epoxy Adhesive Formulations; McGraw-Hill: New York, USA, 2006.
5. *I. Gibson*, *D. W. Rosen*, *B. Stucker*, Additive Manufacturing Technologies, 2., Springer: New York, USA, 2015.
6. *T. D. Ngo*, *A. Kashani*, *G. Imbalzano*, *K. T. Q. Nguyen*, *D. Hui*, Additive manufacturing (3D printing): A review of materials, methods, applications and challenges, Compos. Part B **143** (2018) 172–196, doi: https://doi.org/10.1016/j.compositesb.2018.02.012.
7. *N. Guo*, *M. C. Leu*, Additive manufacturing: technology, applications and research needs, Front. Mech. Eng. **8** (2013) 215–243, doi: https://doi.org/10.1007/s11465-013-0248-8.
8. *R. Chaudhary*, *P. Fabbri*, *E. Leoni*, *F. Mazzanti*, *R. Akbari*, *C. Antonini*, Additive Manufacturing by Digital Light Processing: A Review, Prog. Addit. Manuf. **8** (2023) 331–351, doi: https://doi.org/10.1007/s40964-022-00336-0.

9. *M. Pagac, J. Hajnys, Q. P. Ma, L. Jancar, J. Jansa, P. Stefek, J. Mesicek*, A review of vat photopolymerization technology: materials, applications, challenges, and future trends of 3D printing, Polymers **13** (2021) 598, doi: https://doi.org/10.3390/polym13040598
10. *D. Vrsaljko, M.-P. Marković, I. K. Cingesar, F. Car*, Aditivna proizvodnja u kemijskom inženjerstvu. Prvi dio: procesi za polimere, Kem. Ind. **74** (2025) 43–56, doi: https://doi.org/10.15255/KUI.2024.044
11. *R. Chaudhary, R. Akbari, C. Antonini,* Rational Design and Characterization of Materials for Optimized Additive Manufacturing by Digital Light Processing, Polymers **15** (2023) 287, doi: https://doi.org/10.3390/polym15020287.
12. *S. C. Ligon, R. Liska, J. Stampfl, M. Gurr, R. Mülhaupt*, Polymers for 3D Printing and Customized Additive Manufacturing, Chem. Rev. **117** (2017) 10212–10290 doi: https://doi.org/10.1021/acs.chemrev.7b00074.
13. *D. Wu, Z. Zhao, Q. Zhang, H.J. Qi, D. Fang*, Mechanics of Shape Distortion of DLP 3D Printed Structures During UV Post-Curing, Soft. Mater. **15** (2019) 6151–6159, doi: https://doi.org/10.1039/C9SM00725C.
14. *M. Staffova, F. Ondreas, J. Svatik, M. Zboncak, J. Jancar, P. Lepcio*, 3D printing and post-curing optimization of photopolymerized structures: Basic concepts and effective tools for improved thermomechanical properties, Polymer Testing **108** (2022) 107499, doi: https://doi.org/10.1016/j.polymertesting.2022.107499.
15. *B. Steyrer, P. Neubauer, R. Liska, J. Stampfl*, Visible Light Photoinitiator for 3D-Printing of Tough Methacrylate Resins, Materials **10** (2017) 1445, doi: https://doi.org/10.3390/ma10121445.
16. *H. Gong, M. Beauchamp, S. Perry, A. T. Woolley, G. P. Nordin*, Evaluation of post-curing and laser manufacturing parameters on the properties of SOMOS 7110 photosensitive resin used in stereolithography, Rapid Prototyp. J. **21** (2015) 545–553, doi: https://doi.org/10.1108/RPJ-09-2013-0099.
17. *M. D. Monzón, Z. Ortega, A. Hernández, R. Paz, F. Ortega*, Anisotropy of Photopolymer Parts Made by Digital Light Processing, Materials **10** (2017) 64, doi: https://doi.org/10.3390/ma10010064.
18. *I. K. Cingesar, M. P. Marković, D. Vrsaljko*, Effect of post-processing conditions on polyacrylate materials used in stereolithography, Addit. Manuf. **55** (2022.) doi: https://doi.org/10.1016/j.addma.2022.102813.
19. ISO 527-2:2025. Plastics—Determination of Tensile Properties—Part 2: Test Conditions for Moulding and Extrusion Plastics; International Organization for Standardization (ISO): Geneva, Switzerland, 2025.
20. *X. Wang, M. Jiang, Z. Zhou, J. Gou, D. Hui*, 3D Printing of Polymer Matrix Composites: A Review and Prospective, Compos. Part B Eng. **110** (2017) 442–458, doi: https://doi.org/10.1016/j.compositesb.2016.11.034.
21. *A. Bagheri, J. Jin,* Photopolymerization in 3D Printing, ACS Appl. Polym. Mater. **1** (2019) 593–611, doi: https://doi.org/10.1021/acsapm.8b00165.
22. *H. W. S. Hsieh, B. Post, H. Morawetz*, A Crystallographic Study of Polymers Exhibiting Side-Chain Crystallization, J. Polym. Sci. **14** (1976) 441–457, doi: https://doi.org/10.1002/pol.1976.180140709.
23. *L. Jiang, J. Zhang, M. P. Wolcott,* Comparison of Tensile and Dynamic Mechanical Properties of Injection Molded and 3D Printed ABS, Addit. Manuf. **12** (2016) 31–38, doi: https://doi.org/10.1016/j.addma.2016.06.005.
24. *V. V. Krongauz,* Diffusion in polymers dependence on crosslink density, J. Therm. Anal. Calorim. **102** (2010) 435–445, doi: https://doi.org/10.1007/s10973-010-0922-6.
25. *J. Nam, M. Kim*, Advances in materials and technologies for digital light processing 3D printing, Nano Convergence **11** (2024) 45, doi: https://doi.org/10.1186/s40580-024-00452-3.

SAŽETAK

Utjecaj orijentacije ispisa i naknadne obrade na svojstva predmeta izrađenih tehnologijom digitalne obrade svjetlom

Marijan-Pere Marković, Lara Štorga, Elizabeta Forjan* i *Domagoj Vrsaljko*

Aditivna proizvodnja (3D-ispis) predstavlja postupak izrade trodimenzionalnih predmeta sloj po sloj na temelju digitalnih modela izrađenih računalno potpomognutim dizajnom (CAD). U tehnologiji digitalne obrade svjetlom (DLP) model se pretvara u niz slojeva koji se izrađuju selektivnom fotopolimerizacijom smole pomoću projiciranog svjetla.

U ovom radu istražen je utjecaj uvjeta izrade i naknadnog očvršćivanja na svojstva akrilatne fotopolimerne smole (*AnyCubic 3D Printing UV Sensitive Resin*) primijenjene u DLP 3D ispisu. Analiziran je utjecaj orijentacije ispisa (0°, 45° i 90°) te trajanja naknadnog očvršćivanja (0, 5 i 15 min) u komori valne duljine 405 nm na mehanička, toplinska i kemijska svojstva materijala.

Rezultati ispitivanja pokazali su da orijentacija ispisa i vrijeme naknadnog očvršćivanja znatno utječu na mehaničko ponašanje i kemijsku otpornost materijala. Uzorci ispisani pod kutom od 90° u odnosu na podlogu ispisa pokazali su najveću vlačnu čvrstoću (53,9 MPa) i prekidnu čvrstoću (53,3 MPa), dok su uzorci ispisani pod kutom od 0° imali najveći Youngov modul (1184 MPa). Najveći stupanj bubrenja zabilježen je u acetonu (11 %) i metanolu (10 %), pri čemu se apsorpcija otapala smanjivala s produljenjem vremena naknadnog očvršćivanja. Toplinska analiza pokazala je tek neznatne promjene temperature staklastog prijelaza (49,1 – 53,5 °C), dok FTIR spektri nisu pokazali značajne razlike između različitih uvjeta naknadnog očvršćivanja. Dobiveni rezultati potvrđuju da se mehanička svojstva i kemijska otpornost DLP ispisanih predmeta mogu prilagoditi odabirom odgovarajuće orijentacije ispisa i uvjeta naknadnog očvršćivanja, dok toplinska svojstva ostaju nepromijenjena.

Ključne riječi

Aditivna proizvodnja, digitalna obrada svjetlom, orijentacija ispisa, naknadna obrada

Sveučilište u Zagrebu Fakultet kemijskog inženjerstva i tehnologije, Trg Marka Marulića 19, 10 000 Zagreb

Izvorni znanstveni rad
Prispjelo 15. lipnja 2026.
Prihvaćeno 24. srpnja 2026.